SEMI-BLIND DECONVOLUTION OF NEURAL IMPULSE RESPONSE IN EVENT-RELATED fMRI USING GIBBS SAMPLER

Salima Makni,[1,3] *Philippe Ciuciu,*[1,3] *Jérôme Idier,*[2] *and Jean-Baptiste Poline*[1,3]

[1]Service Hospitalier Frédéric Joliot (CEA) 4, Place du Général Leclerc, 91406 Orsay, France
[2]IRCCyN (CNRS), 1 rue de la Noë, BP 92101 44321 Nantes cedex 3, France
[3] IFR 49, Institut d'Imagerie Neurofonctionnelle, Paris, France
[1] name@shfj.cea.fr, [2] Jerome.Idier@irccyn.ec-nantes.fr

ABSTRACT

Identification of the Hemodynamic Response Function (HRF) in functional Magnetic Resonance Imaging (fMRI) is essential for a better understanding of cerebral activity. In a given region-of-interest (ROI) of the brain, several works have demonstrated that neighbor voxels have close shape responses, but with potentially different magnitude. This property of similarity also holds between HRFs corresponding to different stimuli in the paradigm. In this paper, we account for these features in a given ROI and estimate a single HRF shape but several magnitude coefficients per voxel and condition, which may be thought of representing the neural response level. Identified as a *semi-blind deconvolution* inverse problem, we use a Gibbs sampling approach to estimate the unknown quantities. Our method, validated both on synthetic and real fMRI data provides spatial activation maps in a given ROI with no assumptions on the exact shape of the HRF.

1. INTRODUCTION

The end goal of fMRI is to detect and localize dynamic brain processes for various stimulations or tasks [1]. In recent works [2, 3], the authors have developed an unsupervised robust non-parametric method for HRF estimation. They observed that the shape of the response tends to be spatially homogeneous. Here, we propose an extension that takes this feature into account. Our purpose is therefore to estimate a single HRF shape in a given ROI and a magnitude coefficient for each voxel and stimulus type. This coefficient may better represent the neural response level. The problem can be formulated as a *semi-blind deconvolution* inverse problem since the arrival times of neural responses are known. To cope with this issue, we develop a Bayesian approach using physiological prior information. The HRF is modeled as a smooth function of time. The stimulus-dependent "neural" magnitudes are assumed to be statistically independent across voxels and between stimulus types. The hyperparameters that govern Gaussian prior distributions as well as the noise variances (one per voxel) have to be estimated in an appropriate way. We also model "physiological" artefacts (drifts) that corrupt real fMRI data. We use the well-known Gibbs sampler algorithm to draw random samples iteratively from the posterior distribution, in order to compute posterior mean estimates. We tested our method on both synthetic and real fMRI data to demonstrate that the proposed model provides a robust estimation of the parameters of interest.

2. PROBLEM FORMULATION

2.1. Standard formulation

The fMRI signal $\boldsymbol{y}_j = \left[y_{t_j,1}, \ldots, y_{t_j,N}\right]^{\mathrm{t}}$ is measured in voxel V_j of the brain at times $(t_n = n\ TR)_{1\leq n\leq N}$, TR being the Repetition Time. Let $(x_t)_{t\geq t_0}$ be the binary sequence coding the time occurrences of the stimuli in the experimental paradigm. Assuming that the neurovascular system is linear and time-invariant, the fMRI data are related to the stimulus sequence as follows:

$$\boldsymbol{y}_j = \boldsymbol{X}\boldsymbol{h}_j + \boldsymbol{P}\boldsymbol{l}_j + \boldsymbol{b}_j, \qquad \text{with } \boldsymbol{b}_j \sim \mathcal{N}(\boldsymbol{0}, \sigma_b^2 \boldsymbol{I}), \quad (1)$$

$\boldsymbol{x}_{t_n} = [x_{t_n}, x_{t_n-\Delta t}, \ldots, x_{t_n-K\Delta t}]^{\mathrm{t}}$, $\boldsymbol{X} = [\boldsymbol{x}_{t_1}, \ldots, \boldsymbol{x}_{t_N}]^{\mathrm{t}}$ and $\boldsymbol{h}_j = [h_{j,0}, h_{j,\Delta t}, \ldots, h_{j,K\Delta t}]^{\mathrm{t}}$. In event-related fMRI, the trials of a stimulus may occur at times that differ from instants of acquisition. Consequently, trials are approximated on a finer temporal grid defined by a sampling period $\Delta t < TR$. In (1), the matrix $\boldsymbol{P} = [P_1, \ldots, P_Q]$ (Q depend on the lowest frequency attributable to the drift term) consists of an orthonormal basis of functions $P_q = [P_q(t_1), \ldots, P_q(t_N)]^{\mathrm{t}}$. This matrix is fixed a priori and models the low frequency drift in the fMRI experiments.

2.2. Spatial extension

In functional neuroimaging, we are primarily interested in detecting functionally homogeneous clusters of voxels involved in the same way in a cognitive task. Once such an homogeneous ROI has been found, we search for the region-based *canonical* time response. To this end, we introduce a generalization of (1) that accounts for voxel-dependent signal and noise levels but assumes a single HRF shape over the region. Let $\mathcal{R} = \{V_1, \ldots, V_J\}$ be the ROI, model (1) becomes:

$$\boldsymbol{y}_j = a_j \boldsymbol{X}\boldsymbol{h} + \boldsymbol{P}\boldsymbol{l}_j + \boldsymbol{b}_j, \quad \forall j \in \{1, \ldots, J\}. \qquad (2)$$

where a_j stands for the "neural" response level in voxel V_j. Following [4], the neurovascular system is assumed *time-invariant*, such that a_j is constant during the experiment.

Several noise models can be considered for $\mathcal{R}$ depending on its spatial properties. The simplest is a zero-mean Gaussian white noise process $\boldsymbol{b}$ of unknown variance $\sigma_{\boldsymbol{b}}^2$, independent of $\boldsymbol{h}$. Nonetheless, due to spatially varying artifacts (*e.g.,* partial volume effect), the noise level may strongly vary from one voxel to another. This requires a slightly more complicated model, in which a specific noise variance σ_j^2 is attributed to each voxel V_j. We should therefore estimate $\boldsymbol{\sigma}^2 = \left[\sigma_1^2, \ldots, \sigma_J^2\right]^{\mathrm{t}}$ as well.

2.3. Multicondition extension

Generally, fMRI experiments consist of several conditions (visual, auditory, ...). We further extend model (2) to estimate neural impulse levels that vary with the stimulus type. Let $(\boldsymbol{X}^m)_{1 \leq m \leq M}$ be the different stimulus-dependent onset matrices, each of them being defined as the previous $\boldsymbol{X}$ matrix. Suppose also that the responses to the different stimuli add in a *linear* way. Then the generalization of (2) is given by:

$$\boldsymbol{y}_j = \sum_{m=1}^{M} a_j^m \boldsymbol{X}^m \boldsymbol{h} + \boldsymbol{P}\boldsymbol{l}_j + \boldsymbol{b}_j, \quad \forall j \in \{1, \ldots, J\}. \quad (3)$$

We are now interested by the joint estimation of the HRF $\boldsymbol{h}$ and the neural response levels $\boldsymbol{A} = (a_j^m)_{1 \leq j \leq J}^{1 \leq m \leq M}$ in region $\mathcal{R}$. To this end, we first need to define the likelihood function. We assume the fMRI time series $\boldsymbol{Y} = [\boldsymbol{y}_1, \ldots, \boldsymbol{y}_J]$ to be statistically independent and identically distributed (iid), such that the likelihood $p(\boldsymbol{Y}|\boldsymbol{h}, \boldsymbol{A}, \boldsymbol{l}, \boldsymbol{\sigma}^2)$ reads:

$$p(\boldsymbol{Y} \,|\, \boldsymbol{h}, \boldsymbol{A}, \boldsymbol{l}, \boldsymbol{\sigma}^2) = \prod_{j=1}^{J} p(\boldsymbol{y}_j \,|\, \boldsymbol{h}, \boldsymbol{A}, \boldsymbol{l}_j, \boldsymbol{\sigma}_j^2)$$

$$\propto \prod_j \sigma_j^{-N} \exp\left(-\sum_j \frac{1}{2\sigma_j^2} \left\| \boldsymbol{y}_j - \sum_m a_j^m \boldsymbol{X}^m \boldsymbol{h} - \boldsymbol{P}\boldsymbol{l}_j \right\|^2\right).$$

Maximum likelihood (ML) estimation of $(\boldsymbol{h}, \boldsymbol{A})$ is a bilinear inverse problem since (3) is linear with respect to $\boldsymbol{h}$ when $\boldsymbol{A}$ is fixed and *vice-versa*. In addition, this problem is ill-posed since the ML solution $(\boldsymbol{h}^*, \boldsymbol{A}^*)$ is not unique. To solve this ill-posed problem, we propose a solution in the Bayesian framework.

3. A SEMI-BLIND DECONVOLUTION APPROACH

3.1. Prior information

The HRF. As physiologically advocated in [5], the HRF can be characterized as follows [3]: *(i)* its variations are smooth; *(ii)* it is causal and returns to a baseline after about 25 sec; its amplitude vanishes at first and end time points. To fulfil conditions *(i)*-*(ii)*, we use a Gaussian distribution $p(\boldsymbol{h}; \sigma_{\boldsymbol{h}}^2, \boldsymbol{R}) = \mathcal{N}(0, \sigma_{\boldsymbol{h}}^2 \boldsymbol{R})$ with $\boldsymbol{R} = (\boldsymbol{D}_2^{\mathrm{t}} \boldsymbol{D}_2)^{-1}$ and $\boldsymbol{D}_2$ is a second-order finite difference matrix, truncated to account for $h_0 = h_{K\Delta t} = 0$.

The "neural" responses. It is reasonable to assume that different types of stimuli induce statistically independent neural responses *i.e.,* $p(\boldsymbol{A}; \boldsymbol{\theta}_{\boldsymbol{A}}) = \prod_m p(\boldsymbol{a}^m; \boldsymbol{\theta}_m)$ with $\boldsymbol{a}^m = [a_1^m, \ldots, a_J^m]$. For condition m, the neural response level is assumed to be $\mathcal{N}(\mu^m, \sigma_m^2)$-distributed. Moreover, vector $\boldsymbol{a}^m$ is a set of independent realizations since we do not model any spatial correlation between the response levels of neighbor voxels.

The low-frequency drift. Vector $\boldsymbol{l} = [\boldsymbol{l}_1^{\mathrm{t}}, \ldots, \boldsymbol{l}_J^{\mathrm{t}}]^{\mathrm{t}}$ defines the unknown weighting coefficients of the basis function $\boldsymbol{P}$. We assume that $\boldsymbol{l}$ is a random process independent of $\boldsymbol{h}$ such that $p(\boldsymbol{l}; \boldsymbol{\sigma}_l^2) = \prod_j p(l_j; \sigma_l^2)$ and $l_j \sim \mathcal{N}(\boldsymbol{0}, \sigma_l^2 \boldsymbol{I}_{Q_j})$. In this paper calculations will be given in the non informative case, that is when $\sigma_l^2 \to +\infty$.

The hyperparameters. The complete set of hyperparameters to be estimated is denoted $\boldsymbol{\Theta} = \left[\boldsymbol{\sigma}^2; \boldsymbol{\theta}_{\boldsymbol{A}}\right]$. It consists of noise variances on the one hand, and location and scaling parameters $\boldsymbol{\theta}_m = (\mu^m, \sigma_m^2)$ of $p(\boldsymbol{a}^m; \boldsymbol{\theta}_m)$ on the other. For every σ_j^2, we resort to non informative priors such as *Jeffreys*' probability distribution function (pdf). Besides, we have set $\sigma_{\boldsymbol{h}}^2 = 1$ to raise the scale ambiguity encountered in blind deconvolution problems [6].

3.2. Posterior distribution

The posterior pdf. The posterior pdf reads:

$$p(\boldsymbol{h}, \boldsymbol{A}, \boldsymbol{l}, \boldsymbol{\Theta}|\boldsymbol{Y}) \propto$$
$$p(\boldsymbol{Y}|\boldsymbol{h}, \boldsymbol{A}, \boldsymbol{l}, \boldsymbol{\sigma}^2)\, p(\boldsymbol{h})\, p(\boldsymbol{A}|\boldsymbol{\theta}_{\boldsymbol{A}})\, p(\boldsymbol{l})\, p(\boldsymbol{\theta}_{\boldsymbol{A}})\, p(\boldsymbol{\sigma}^2).$$

Since vector $\boldsymbol{l}$ embodies nuisance variables that can be easily integrated out, we prefer to generate realizations of the marginal distribution $p(\boldsymbol{h}, \boldsymbol{A}, \boldsymbol{\Theta} \,|\, \boldsymbol{Y}) = \int p(\boldsymbol{h}, \boldsymbol{A}, l, \boldsymbol{\Theta} | \boldsymbol{Y})\, dl$, so that the number of parameters to be sampled is reduced.

The Gibbs sampler. Gibbs sampling has already been applied in the context of blind deconvolution problems [6]. It is an appropriate algorithm to get realizations of a pdf of interest, here $p(\boldsymbol{h}, \boldsymbol{A}, \boldsymbol{\Theta} \,|\, \boldsymbol{Y})$. It consists in building a Markov chain whose target distribution is $p(\boldsymbol{h}, \boldsymbol{A}, \boldsymbol{\Theta} \,|\, \boldsymbol{Y})$, by sequentially generating random samples from the conditional distribution $p(\boldsymbol{h}|\boldsymbol{Y}, \boldsymbol{A}, \boldsymbol{\Theta})$ and $p(\boldsymbol{A}|\boldsymbol{Y}, \boldsymbol{h}, \boldsymbol{\Theta})$. Finally, we compute posterior mean (PM) estimates of ($\boldsymbol{h}$,$\boldsymbol{A}$). For hyperparameters $\boldsymbol{\Theta}$, we also resort to posterior mean estimates.

Computational details. The conditional posterior distribution of $\boldsymbol{h}$, $\boldsymbol{A}$ and $\boldsymbol{\Theta}$ is simply proportionnal to $p(\boldsymbol{h}, \boldsymbol{A}, \boldsymbol{\Theta}|\boldsymbol{Y})$. We get

$$p(\boldsymbol{h}|\boldsymbol{Y}, \boldsymbol{A}, \boldsymbol{\sigma}^2) \sim \mathcal{N}(m_{\boldsymbol{h}}, \boldsymbol{\Sigma}_{\boldsymbol{h}}), \tag{4}$$

$$\boldsymbol{\Sigma}_{\boldsymbol{h}}^{-1} = \boldsymbol{R}^{-1} + \sum_j \frac{1}{\sigma_j^2} \Big\| \sum_m a_j^m \boldsymbol{X}^m \Big\|^2 - \frac{1}{\sigma_j^2} \Big\| \boldsymbol{P}^{\mathrm{t}} \sum_m a_j^m \boldsymbol{X}^m \Big\|^2$$

$$m_{\boldsymbol{h}} = \boldsymbol{\Sigma}_{\boldsymbol{h}} \sum_j \frac{1}{\sigma_j^2} \Big(\sum_m a_j^m \boldsymbol{X}^m \Big)^{\mathrm{t}} (\boldsymbol{I}_N - \boldsymbol{P}\boldsymbol{P}^{\mathrm{t}}) \boldsymbol{y}_j,$$

$$p(\boldsymbol{A}|\boldsymbol{Y}, \boldsymbol{h}, \boldsymbol{\sigma}^2) = \prod_j \big[p(\boldsymbol{a}_j | \boldsymbol{y}_j, \boldsymbol{h}, \sigma_j^2) \sim \mathcal{N}(m_{\boldsymbol{a}_j}, \boldsymbol{\Sigma}_{\boldsymbol{a}_j}) \big] \tag{5}$$

$$\boldsymbol{\Sigma}_{\boldsymbol{a}_j}^{-1} = \frac{1}{\sigma_j^2} \mathbb{X}^{\mathrm{t}} (\boldsymbol{I}_N - \boldsymbol{P}\boldsymbol{P}^{\mathrm{t}}) \mathbb{X} + \mathrm{diag}\left[\sigma_1^{-2}, \cdots, \sigma_M^{-2} \right]$$

$$m_{\boldsymbol{a}_j} = \boldsymbol{\Sigma}_{\boldsymbol{a}_j} \left(\frac{1}{\sigma_j^2} \mathbb{X}^{\mathrm{t}} (\boldsymbol{I}_N - \boldsymbol{P}\boldsymbol{P}^{\mathrm{t}}) \boldsymbol{y}_j + \left[\frac{\mu^1}{\sigma_1^2}, \cdots, \frac{\mu^M}{\sigma_M^2} \right]^{\mathrm{t}} \right)$$

$$p(\sigma_j^2 | \boldsymbol{y}_j, \boldsymbol{h}, \boldsymbol{a}_j) \sim \mathcal{IG}(N/2 - Q_j/2, \boldsymbol{\beta}), \tag{6}$$

$$\boldsymbol{\beta} = \frac{1}{2} \Big\| \boldsymbol{y}_j - \sum_m a_j^m \boldsymbol{X}^m \boldsymbol{h} \Big\|^2 - \frac{1}{2} \Big\| \boldsymbol{y}_j - \sum_m a_j^m \boldsymbol{X}^m \boldsymbol{h} \Big\|^2_{\boldsymbol{P}\boldsymbol{P}^{\mathrm{t}}}$$

where $\mathbb{X} = [\boldsymbol{X}^1 \boldsymbol{h} \,|\, \cdots \,|\, \boldsymbol{X}^M \boldsymbol{h}]$. To estimate μ^m and σ_m^2, we use the following proposition (*cf.* [7, p. 187]): If vector $\boldsymbol{a}^m$ is a set of $\mathcal{N}(\mu^m, \sigma_m^2)$-distributed iid observations, the posterior distribution of (μ^m, σ_m^2) associated with the prior distribution $\widetilde{\pi}(\mu^m, \sigma_m) = \sigma_m^{-1}$ is:

$$p(\mu^m \,|\, \sigma_m^2, \overline{\boldsymbol{a}}^m, s^2) \sim \mathcal{N}(\overline{\boldsymbol{a}}^m, \sigma_m^2 / J) \tag{7}$$

$$p(\sigma_m^2 \,|\, \overline{\boldsymbol{a}}^m, s^2) \sim \mathcal{IG}((J-1)/2, s^2/2) \tag{8}$$

where $\overline{\boldsymbol{a}}^m = \sum_{j=1}^J a_j^m / J$ and $s^2 = \sum_{j=1}^J (a_j^m - \overline{\boldsymbol{a}}^m)^2$ are sufficient statistics. We summarize the Gibbs sampling algorithm as follows:

(1) Initialization: choose $\boldsymbol{h}^0, \boldsymbol{A}^0, (\boldsymbol{\sigma}^2)^0, \boldsymbol{\theta}_{\boldsymbol{A}}^0$.

(2) Iteration k: draw samples $\boldsymbol{h}^k, \boldsymbol{A}^k, (\boldsymbol{\sigma}^2)^k, \boldsymbol{\theta}_{\boldsymbol{A}}^k$ from the conditional posterior distributions (4)-(8).

(3) Iterate until maximum iteration number K_0 is achieved.

Finally, we compute posterior mean estimates using the following approximation:[1]

$$\widehat{\theta}^{\mathrm{PM}} = \sum_{k=I}^{K_0} \theta^k / (K_0 - I + 1),\ \forall \theta \in \{ \boldsymbol{h}, \boldsymbol{A}, \boldsymbol{\sigma}^2, \boldsymbol{\mu}_{\boldsymbol{a}}, \boldsymbol{\sigma}_{\boldsymbol{a}}^2 \}$$

4. SIMULATION RESULTS

We simulated a random inter mixed sequence of indexes coding for $M = 2$ stimuli. The inter-stimulus intervals (ISIs) between successive trials were random and uniformly distributed on [1.5, 2.5]. A sampling period of $\delta t = 0.5$ s was chosen for the onsets of the trials. Scale factors $a^1_{1,\ldots,10}$ and $a^2_{1,\ldots,10}$ were $\mathcal{N}(\mu^1 = 3, \sigma_1^2 = 0.5)$, $\mathcal{N}(\mu^2 = 10, \sigma_2^2 = 0.2)$-distributed, respectively. In all voxels ($J = 10$), the time series related to a given stimulus type was convolved with a canonical HRF $\boldsymbol{h}_c$ (used by the SPM99 toolbox[2]). The shape of this function is plotted in Fig 1(a) as a dotted line. A realistic white Gaussian noise ($\forall j, \sigma_j^2 = 0.3$) and a $\mathcal{N}(\boldsymbol{0}_Q, \boldsymbol{I}_Q)$-distributed low-frequency drift, whose cut-off-period is 70 s, were added.

Fig 1(b)-(c) show the estimated neural response levels for both conditions in all voxels. These estimates accurately match the true values. The HRF estimate plotted as a solid line in Fig 1(a) is very close to $\boldsymbol{h}_c$.

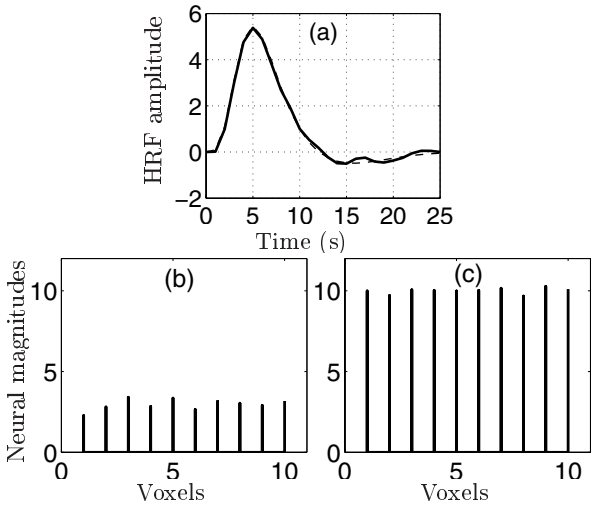

Fig. 1. (a) true HRF (- -) and ROI-based HRF estimate (–), (b)-(c) respectively estimates of neural response levels a^1 and a^2.

[1] Samples $\theta^1, \ldots, \theta^I$ are discarded: they correspond to a so-called *burn-in* period.

[2] `www.fil.ion.ucl.ac.uk/spm/spm99.html`

5. RESULTS ON REAL FMRI DATA

The method was assessed on real data acquired in a speech discrimination experiment that consisted of $I = 6$ sessions comprising $N = 100$ trials lasting 3.3 seconds each (for this test, we just used data relative to the first session). In each trial, the participant heard two pseudo-words over headphones. His task was to indicate whether he had perceived or not a difference between the two stimuli. There were $M = 4$ types of trials: 'Silence' (noise scanner), 'Phonological', 'Acoustic', 'Control'. In trials belonging to the 'Control' condition, the two auditory stimuli in the pair were exactly the same. In the 'Phonological' condition, the stimuli differed along a contrast used to distinguish words in the language of the participant. In the 'Acoustic' condition, the stimuli also differed but the contrast between the stimuli was not relevant to the language of the participant. In Fig. 2(b), the circles indicate the ROI in one subject, located in the primary auditory cortex. The ROI comprised 7 voxels in three slices. The fMRI data were extracted using the MARSBAR toolbox[3]. The ROI-based HRF estimate is plotted in Fig. 2(a) and the estimated neural magnitudes for each condition are represented in Fig. 2(c)-(f). Within a given condition, the magnitudes are almost the same for all voxels, but their amplitude varies with conditions. This is the case for this small ROI but others results show a variation in space of the HRF magnitude.

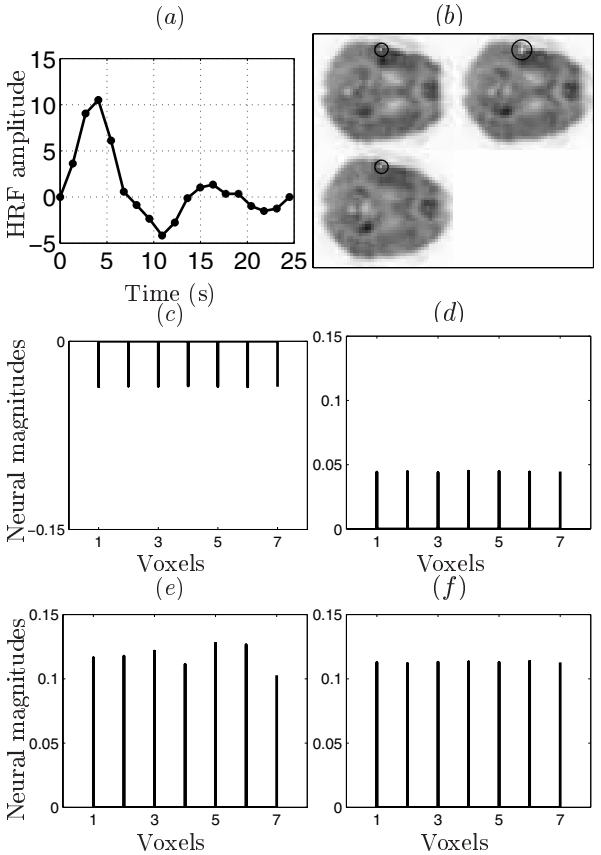

Fig. 2. (a) ROI-based HRF estimate, (b) The ROI $\mathcal{R} = \{V_1, \ldots, V_7\}$, (c)-(f) estimates of neural response levels $\boldsymbol{a}^1$, $\boldsymbol{a}^2$, $\boldsymbol{a}^3$ and $\boldsymbol{a}^4$.

6. CONCLUSION

We have proposed an original method for semi-blind deconvolution of impulse neural response in functional neuroimaging. This method extends previous work [3] to deal with regional HRF estimation in an efficient way while modeling the spatial variability of the neural response for each type of stimulus. We have validated this approach on both synthetic and real fMRI data. Finally, an interesting extension of our method would consist in modeling spatial correlation of the neural response levels with a 3D anisotropic Markov random field to account for MRI acquisition.

7. REFERENCES

[1] P. A. Bandettini, A. Jesmanowicz, E. C. Wong, and J. S. Hyde, "Processing strategies for time-course data sets in functional MRI of the human brain," *Magn. Reson. Med.*, vol. 30, pp. 161–173, 1993.

[2] G. Marrelec, H. Benali, P. Ciuciu, and J.-B. Poline, "Bayesian estimation of the hemodynamic response function in functional MRI," in *Bayesian Inference and Maximum Entropy Methods*, R. Fry, Ed. Baltimore, MD: MaxEnt Workshops, August 2001.

[3] P. Ciuciu, J.-B. Poline, G. Marrelec, J. Idier, C. Pallier, and H. Benali, "Unsupervised robust non-parametric estimation of the hemodynamic response function for any fMRI experiment," *IEEE Trans. Medical Imaging*, vol. 22, no. 10, pp. 1235–1251, Oct. 2003.

[4] G. H. Glover, "Deconvolution of impulse response in event-related BOLD fMRI," *Neuroimage*, vol. 9, pp. 416–429, 1999.

[5] R. Buxton and L. Frank, "A model for the coupling between cerebral blood flow and oxygen metabolism during neural stimulation," *J. Cereb. Blood Flow Metab.*, vol. 17, no. 1, pp. 64–72, 1997.

[6] Q. Cheng, R. Chen, and T.-H. Li, "Simultaneous wavelet estimation and deconvolution of reflection seismic signals," *IEEE Trans. Geosci. Remote Sensing*, vol. 34, pp. 377–384, Mar. 1996.

[7] C. P. Robert, *The Bayesian Choice. Second Edition*, Springer Texts in Statistics. Springer Verlag, NY, 2001.

[3] `www.marsbar.sourceforge.net`